

See discussions, stats, and author profiles for this publication at: <https://www.researchgate.net/publication/266912661>

Ground and Excited State Proton Transfer of the Bioactive Plant Flavonol Robinetin in a Protein Environment: Spectroscopic and Molecular Modeling Studies

ARTICLE *in* THE JOURNAL OF PHYSICAL CHEMISTRY B · OCTOBER 2014

Impact Factor: 3.3 · DOI: 10.1021/jp508410v

CITATION

1

READS

44

4 AUTHORS, INCLUDING:



[Sudip Chaudhuri](#)

Gandhi Centenary B. T. CollegeHabra, India

13 PUBLICATIONS 313 CITATIONS

[SEE PROFILE](#)



[Sandipan Chakraborty](#)

Indian Association for the Cultivation of Science

31 PUBLICATIONS 208 CITATIONS

[SEE PROFILE](#)



[Pradeep K Sengupta](#)

University of Calcutta

56 PUBLICATIONS 1,921 CITATIONS

[SEE PROFILE](#)

Ground and Excited State Proton Transfer of the Bioactive Plant Flavonol Robinetin in a Protein Environment: Spectroscopic and Molecular Modeling Studies

Biswa Pathik Pahari,[†] Sudip Chaudhuri,[‡] Sandipan Chakraborty,[§] and Pradeep K. Sengupta*,^{||}

[†]Biophysics and Structural Genomics Division, Saha Institute of Nuclear Physics, 1/AF, Bidhannagar, Kolkata 700064, India

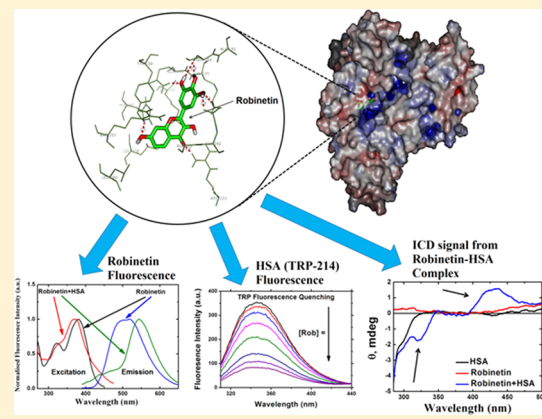
[‡]Gandhi Centenary B. T. College, Habra, Habra-Prafullanagar-743268, India

[§]Department of Microbiology, University of Calcutta, 35 Ballygunge Circular Road, Kolkata 700019, India

^{||}Department of Biophysics, Molecular Biology & Bioinformatics, University of Calcutta, 92 Acharya Prafulla Chandra Road, Kolkata 700009, India

Supporting Information

ABSTRACT: We performed spectroscopic and molecular modeling studies to explore the interaction of the bioactive plant flavonol robinetin ($(3,7,3',4',5'-OH$ flavone), with the carrier protein human serum albumin (HSA). Multiparametric fluorescence sensing, exploiting the intrinsic “two color” fluorescence of robinetin (comprising excited state intramolecular proton transfer (ESIPT) and charge transfer (CT) emissions) reveals that binding to HSA significantly affects the emission and excitation profiles, with strongly blue-shifted (~29 nm) normal fluorescence and remarkable increase in the ESIPT fluorescence anisotropy (r) and lifetime (τ). Flavonol-induced HSA (tryptophan) fluorescence quenching data yield the dynamic quenching constant (K_D) as $5.42 \times 10^3 \text{ M}^{-1}$ and the association constant (K_s) as $5.59 \times 10^4 \text{ M}^{-1}$. Time-resolved fluorescence anisotropy decay studies show dramatic (~170 times) increase in the rotational correlation time (τ_{rot}), reflecting greatly enhanced restrictions in motion of robinetin in the protein matrix. Furthermore, prominent induced circular dichroism (ICD) bands appear, indicating that the chiral environment of HSA strongly perturbs the electronic transitions of the intrinsically achiral robinetin molecule. Molecular docking calculations suggest that robinetin binds in subdomain IIA of HSA, where specific interactions with basic residues promote ground state proton abstraction and stabilize an anionic species, which is consistent with spectroscopic observations.



1. INTRODUCTION

Flavonols (3-hydroxyflavones) are an important class of bioactive naturally occurring phenolic compounds of the flavonoid group, which are ubiquitous in higher plants and abundantly present in common plant-based food and beverages.^{1,2} From the photophysical context, interest in these molecules centers around the fact that they undergo a photoinduced excited state intramolecular proton transfer (ESIPT) reaction (via the internal hydrogen bond linking the C=O and 3-OH groups), resulting in the transformation of the initially excited (N^*) state to the tautomer (T^*) form^{3–6} (see Scheme 1). This reaction is ultrafast (occurring with a time constant of 35 fs for 3-hydroxyflavone in typical aprotic solvents⁷) and extraordinarily sensitive to external hydrogen bonding perturbation of the environment on the internal hydrogen bond of the molecules.⁴ The latter feature leads to “two color” fluorescence emission from the N^* and T^* states, the relative contributions between the two colors being strongly modulated by the local environment. Furthermore, in 3-hydroxyflavone derivatives where the N^* form shows a strong

charge transfer (CT) character, solvent dipolar relaxation plays a prominent role. In such situations, while the yellow-green tautomer (T^*) fluorescence functions as a “proton transfer” probe (sensing H-bonding effects), the blue-violet normal (N^*) fluorescence serves as a “polarity probe” (sensing polarity of the fluorophore environment), which enables multiparametric use of the same fluorophore.^{8–11}

Since the occurrence of ESIPT in such molecules was first proposed more than 3 decades ago,³ over the years, flavonols (comprising 3-hydroxyflavone (3HF) and its natural as well as synthetic derivatives) have emerged as one of the best known group of molecules serving as prototypes for exploring mechanistic aspects of photoinduced ESIPT, the interplay

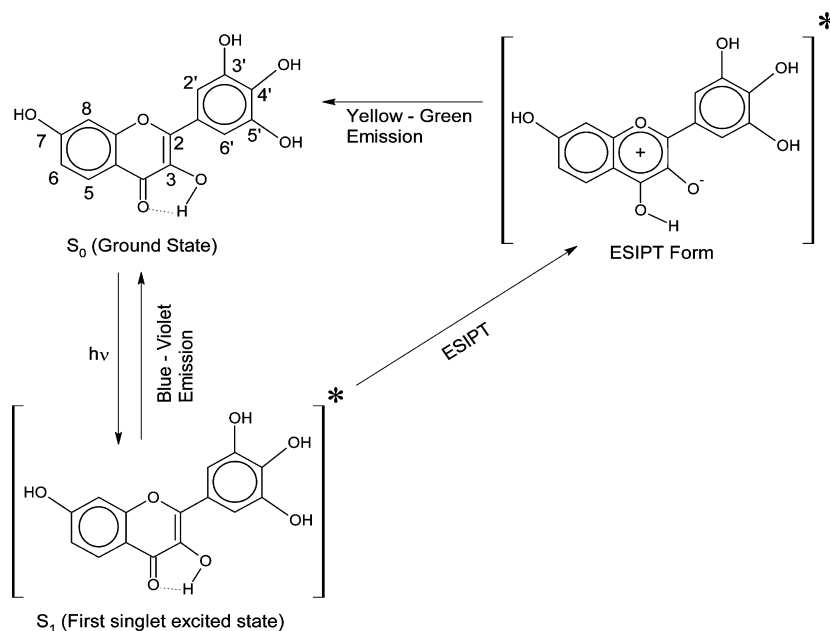
Special Issue: Photoinduced Proton Transfer in Chemistry and Biology Symposium

Received: August 20, 2014

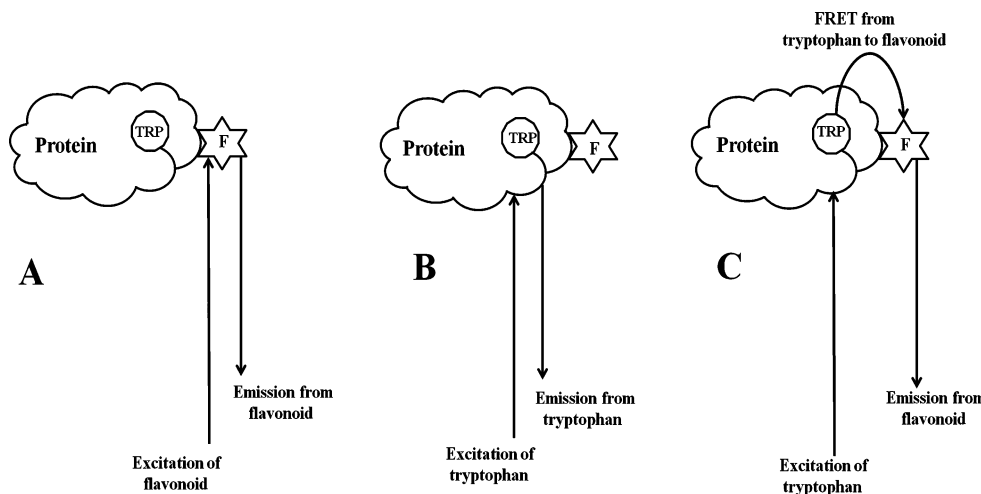
Revised: October 12, 2014

Published: October 14, 2014

Scheme 1. Chemical Structure of the Plant Flavonol, Robinetin, Showing Excited State Intramolecular Proton Transfer (ESIPT) Reaction and “Two Color” Fluorescence Emission



Scheme 2. Schematic Diagrams Depicting Three Different Approaches for Exploring Protein–Flavonoid Interactions via Fluorescence Spectroscopy: (A) Excitation and Detection of Flavonoid Fluorescence, (B) Excitation and Detection of Protein (Tryptophan) Fluorescence, and (C) Excitation of Tryptophan and Detection of Flavonoid Fluorescence via FRET. Adapted from ref 49.



between ESIPT and CT reactions, and two color fluorescence phenomena.^{8,11–15} On a different scenario, flavonols and related flavonoid derivatives (of which >6000 chemically distinct compounds have been identified in plants²) have gained remarkable prominence as powerful antioxidants and promising drugs with novel medicinal properties. They are active against a wide range of free radical mediated and other human diseases (including cancer, cardiovascular ailments, atherosclerosis, ischemia, diabetes, neuronal degeneration, Alzheimer's disease, and AIDS). The high potency and low cytotoxicity of these compounds make them potentially viable alternatives to conventional therapeutics.^{16–21} In this connection, the question of their physiological targets and the mode of interaction with such targets loom large. Motivated by this aspect, we, as well as other groups, have carried out several

studies demonstrating interesting uses of the exquisitely sensitive intrinsic fluorescence of representative flavonols, for exploring their binding properties in potential biorelevant targets (related to therapeutic actions), namely, proteins, biomembranes, duplex as well as quadruplex DNA, and nanovehicles for drug delivery.^{8,10,22–38} There is ample evidence, from both *in vitro* and *in vivo* studies, which suggest that various proteins (including enzymes) frequently serve as receptors for therapeutically active flavonoids of both natural and synthetic origin.^{22,23} Most particularly, studies on the interaction of flavonoids with human serum albumin (HSA, which is the most abundant protein in human blood plasma) are especially relevant since HSA is the principal carrier protein, which plays a critical role in the transport and disposition of flavonoids and other bioactive compounds of therapeutic

importance.^{23,24,39} Furthermore, structural features and substitution patterns on the flavone moiety (such as hydroxylation and glycosylation) strongly modulate the affinity of flavonoids to serum albumins, thus controlling their bioavailability.^{40,41}

In the present study, we have explored the interactions of the plant flavonol, robinetin (3,7,3',4',5'-OH flavone) with HSA, employing electronic absorption, steady state, and time-resolved fluorescence (including lifetime and anisotropy decay measurements), near- and far-UV circular dichroism (CD) spectroscopy, together with computational (molecular docking) studies. Robinetin is a plant flavonol which exhibits ESIPT and two color fluorescence behavior (see Scheme 1).⁹

Moreover, it is gaining increasing attention for its interesting biological activities and multifunctional therapeutic potential (including antioxidant, anticancer, antileishmanial, and anti-mutagenetic actions).^{42–44} Some flavonoids, including robinetin, have also been found to inhibit non-enzymatic glycosylation of hemoglobin, making these potentially useful antidiabetic drugs.^{45–47} Robinetin has close similarity in chemical structure and spectral features with the antioxidant dietary flavonol, fisetin (3,7,3',4'-OH flavone). Like fisetin, its normal fluorescence possesses pronounced CT character⁸ and, hence, shows sensitivity to the environmental polarity⁹ (in contrast to the parent molecule 3HF, where the normal fluorescence emission maximum remains essentially invariant with environmental polarity change⁸), thus providing multiparametric probing opportunities via simultaneous use of the ESIPT and CT emissions.^{8,9} In addition to exploiting the intrinsic two color fluorescence of the flavonol, we also explored flavonoid-induced quenching of the HSA tryptophan fluorescence (arising from the unique Trp-214 residue⁴⁸). This provides an alternative mode for fluorescence sensing of protein–flavonoid interactions, (see Scheme 2), and has proved to be particularly useful for obtaining quantitative data on binding affinity and related parameters.^{49–54} We further report that, apart from the intrinsic photoinduced ESIPT, ground state proton abstraction (presumably by basic residues of HSA) generates an anionic species of robinetin, which is evident from characteristic spectroscopic signatures of the anion observed in the absorption and fluorescence emission and excitation profiles, and predicted by molecular docking studies. To our knowledge, the present report describes for the first time, a detailed spectroscopic study, in combination with molecular modeling calculations, providing critical insights regarding the binding characteristics of robinetin in HSA, offering perspectives for the application of this flavonol as a promising multiwavelength fluorescence probe.

2. MATERIALS AND METHODS

2.1. Chemicals. Robinetin (Extrasynthese, Genay, France) and human serum albumin (HSA, a Sigma-Aldrich product) were used as received. All solvents were of spectroscopic quality.

2.2. Spectroscopic Measurements. Steady state absorption and fluorescence spectra were recorded with a Cecil model 7500 spectrophotometer and Varian Cary-Eclipse spectrofluorometer, respectively. The fluorescence readings were taken by exciting the samples and measuring the emissions, at appropriate wavelengths, and appropriate water/buffer blanks were subtracted from respective measurements. Quartz cuvettes of 1 cm path length were used in all absorption and fluorescence measurements. The fluorescence spectra reported are uncorrected for the wavelength dependence of the

sensitivity of the apparatus. For steady state fluorescence titrations, three independent measurements were performed. Values of Stern–Volmer and bimolecular quenching constant are expressed as mean \pm SD for three independent measurements. “Origin” (version 8.0)⁵⁵ software was used for plotting and fitting purpose and “fitlyk” (version 0.9.8)⁵⁶ was used to deconvolute absorption and fluorescence spectra.

The steady state fluorescence anisotropy (r) values were obtained using the expression,

$$r = \frac{I_{VV} - GI_{VH}}{I_{VV} + 2GI_{VH}} \quad (1)$$

where I_{VV} and I_{VH} are the vertically and horizontally polarized components of probe emission with excitation by vertically polarized light at the respective wavelength and G defines the instrumental correction factor (polarization characteristics of the photometric system) calculated as,⁵⁴

$$G = I_{HV}/I_{HH} \quad (2)$$

Each intensity value used in this expression represents the computer-averaged values of 10 successive measurements.

Time-resolved fluorescence decay measurements were carried out with a Jobin-Yvon nanosecond time correlated single photon counting (TCSPC) spectrometer, using 295 nm (nano-light emitting diode (nano-LED); pulse full width at half-maximum (fwhm) \sim 750 ps) and 375 nm (laser diode; pulse fwhm \sim 120 ps) excitation sources. An emission monochromator was used to block the scattered light and isolate the emissions. Fluorescence intensity decay curves were deconvoluted with the instrument response function and fitted to a multiexponential decay function,

$$F(t) = \sum_i \alpha_i \exp(-t/\tau_i) \quad (3)$$

where $F(t)$ represents the fluorescence intensity at time t and α_i and τ_i are the amplitudes and decay times of the individual components in the multiexponential decay profile such that $\sum_i \alpha_i = 1$. The goodness of fit was estimated by using χ^2 values. Average lifetimes $\bar{\tau}$ were calculated from the decay times and preexponential factors using the expression:⁵⁴

$$\bar{\tau} = \frac{\sum_i \alpha_i \tau_i^2}{\sum_i \alpha_i \tau_i} \quad (4)$$

For measurement of fluorescence depolarization kinetics the parallel (I_{VV}) and perpendicular (I_{VH}) components were collected as a function of time in an alternating manner until the difference of fluorescence counts collected reached \sim 5000. The time-dependent fluorescence anisotropy values $r(t)$ were calculated using the expression:⁵⁴

$$r(t) = \frac{I_{VV}(t) - GI_{VH}(t)}{I_{VV}(t) + 2GI_{VH}(t)} \quad (5)$$

where I_{VV} , I_{VH} , and G are defined the same as for the steady state anisotropy measurements. When freely rotating spherically symmetrical molecules are excited with polarized light, anisotropy decays as a function of time according the following equation

$$r(t) = r_0 e^{-t/\tau_{rot}} \quad (6)$$

where r_0 is the limiting anisotropy, which is the anisotropy value just after photoexcitation (i.e., at $t = 0$) and τ_{rot} is the

rotational correlation time, which is a parameter of molecular rotation (i.e., how fast or slow the molecule rotates in the environment).⁵⁴ Rotational diffusion depolarizes the fluorescence anisotropy from the initial r_0 value to a final randomized value r_∞ . The software DAS6 was used to analyze the fluorescence lifetime and anisotropy decay results.

Circular dichroism spectra were acquired with a Biologic Science Instruments (Claix, France) spectropolarimeter, using rectangular cuvettes with path lengths of 1 mm and 10 mm respectively for the far-UV and near-UV spectral regions. The scan rate was 60 nm/min, and five consecutive spectra were averaged to produce the final spectrum.

All spectral measurements were carried out at room temperature (298 K).

2.3. Molecular Modeling. Molecular modeling studies were carried out to obtain detailed insights into the interactions of robinetin with HSA. Three-dimensional (3-D) atomic coordinates of the protein were obtained from the Brookhaven Protein Data Bank (PDB id 1BM0). All the heteroatoms were removed (including ordered water molecules), and hydrogen atoms were added such that the ionization states of the residues corresponded to neutral pH. Kollman united-atom charge model was applied to the protein, and nonpolar hydrogens were merged. Atomic solvation parameters and fragmental volumes were also added to the protein. A grid map of $126 \times 126 \times 126$ grid points with a grid-point spacing of 0.375 \AA was considered in this study. The map was centered such that it covered the entire functional binding site of HSA. The 3-D structure of robinetin was built using the molecular builder module of HYPERCHEM 7.5⁵⁷ and optimized using AM1 semiempirical method to an root mean square (rms) convergence of 0.001 kcal/mol with Polak-Ribiere conjugate gradient algorithm implemented in the HYPERCHEM 7.5 package.⁵⁷ Rotatable bonds were assigned to the ligand. Partial atomic charges were calculated using Gasteiger–Marsili method, and nonpolar hydrogens were merged. Molecular docking was performed using a Lamarkian genetic algorithm (LGA) which is a genetic algorithm with an adaptive local search method implemented in AutoDock 4.0.⁵⁸ 500 docking runs were carried out, and for each run, a maximum of 2,500,000 GA operations were performed on a single population of 150 individuals. The weights for crossover, mutation, and elitism were default parameters (0.80, 0.02, and 1, respectively). Electrostatic surface potential of the HSA–robinetin complex was generated by solving the Poisson–Boltzmann equation using PBEQ Solver implemented in the CHARMM-GUI web interface.^{59–61} Values for salt concentration (0.15), interior dielectric (2.0), and exterior dielectric (80.0) were chosen to calculate electrostatic surface potential.

3. RESULTS AND DISCUSSION

3.1. Spectroscopic Studies. **3.1.1. Electronic Absorption and Fluorescence Studies of Robinetin.** The electronic absorption behavior of robinetin in the presence of HSA is depicted in Figure 1. The corresponding spectrum in aqueous buffer is also included for reference. In aqueous buffer, the lowest energy characteristic absorption maximum for the neutral robinetin species appears at ~ 360 nm.

In the presence of the protein there is a significant contribution of a long-wavelength absorption band (with maximum at ~ 415 nm) presumably due to enhanced formation of the conjugate anion (which is present only in very small amounts in the aqueous solution in the absence of added

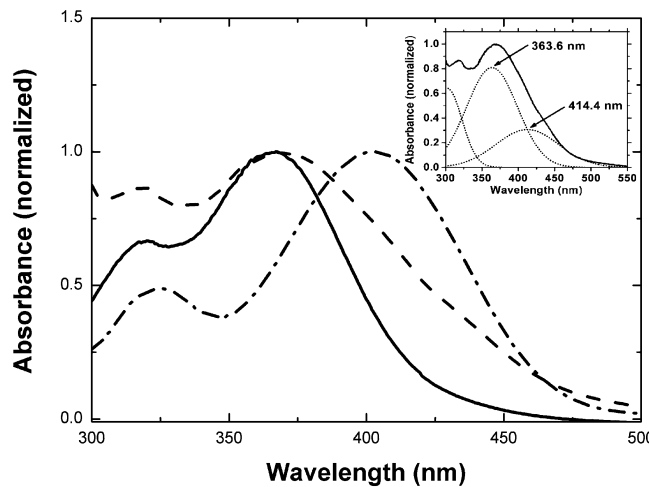


Figure 1. Absorption spectra of robinetin ($5 \mu\text{M}$) in the absence (—) and presence of HSA (--) and of free robinetin in dilute aqueous NaOH solution (pH 9.0; ---). The absorbance values in different environments have been normalized at their respective maxima. Inset: Absorption spectrum of robinetin in the presence of HSA (—) is deconvoluted to identify the different absorbing components, where (---) represent the deconvoluted bands.

protein). This is further verified from its occurrence at alkaline pH in aqueous buffer (Figure 1) as well as from fluorescence studies described later. Thus, two distinct species of robinetin, namely, the neutral (RN) and the anionic (RA) forms, occur in the presence of HSA. Because of the pronounced long-wavelength absorption (assigned to the anionic species of robinetin) in the HSA environment as well at alkaline pH, we infer that the anionic form is generated by HSA-mediated deprotonation of the 3-OH group of robinetin molecule in the ground state. This conclusion derives additional credence from the deconvoluted absorption spectra (Figure 1, inset) which clearly show that there are two absorption bands with maxima at 364 nm (that of the neutral form) and 414 nm (due to the anionic form). The spectral behavior of robinetin observed here is consistent with that reported previously for other structurally related flavonoids in protein environments.^{22–24,34,35,62}

There are three different approaches for exploring protein–flavonoid interactions via fluorescence spectroscopy which involve the following: (a) excitation and detection of intrinsic flavonoid fluorescence, (b) excitation and detection of intrinsic protein (tryptophan) fluorescence, and (c) excitation of the protein (tryptophan) and detection of flavonoid fluorescence via Förster resonance energy transfer (FRET)^{6,54} (see Scheme 2).⁴⁹ Figure 2 presents the normalized fluorescence emission and excitation spectra of robinetin in the presence and absence of HSA. In the presence of HSA, with 360 nm excitation, the emission spectrum of robinetin consists of two color fluorescence bands, namely, a yellow-green emission band along with a high energy band in the blue-violet region. While the blue-violet fluorescence is assigned to the $S_1(\pi\pi^*) \rightarrow S_0$ normal (non-proton-transferred) emission from N^* (non-proton-transferred) species, the large Stokes shifted green fluorescence is attributable to emission from a tautomer (T^*) species generated by an ESIPT process occurring along the internal H-bond (i.e., $\text{C}(4)=\text{O}\cdots\text{HO}-\text{C}(3)$) of the molecule^{3,4,9} (Scheme 1).

The tautomer emission of flavonols is known to be highly sensitive to external hydrogen bonding perturbation, which can

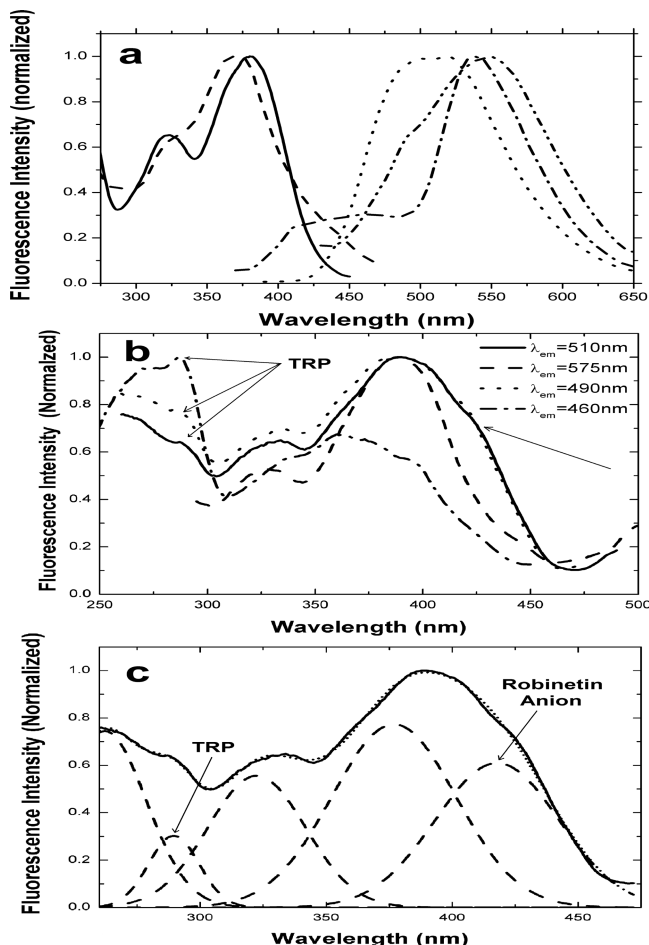


Figure 2. (a) Fluorescence excitation and emission spectra of 5 μM robinetin in neutral aqueous buffer with $\lambda_{\text{em}} = 520 \text{ nm}$ (—) and $\lambda_{\text{ex}} = 360 \text{ nm}$ (···) and in the presence of 25 μM HSA with $\lambda_{\text{ex}} = 360 \text{ nm}$ (---), $\lambda_{\text{em}} = 520 \text{ nm}$ (--) and $\lambda_{\text{ex}} = 420 \text{ nm}$ (····). The emission intensities in different environments have been normalized at the respective maximum. (b) Fluorescence excitation spectra of robinetin–HSA complex recorded at various emission wavelengths. (c) Deconvoluted fluorescence excitation spectrum of robinetin ($\lambda_{\text{em}} = 510 \text{ nm}$) (—) in the presence of HSA to identify various emitting components (--), where (···) represents the fitted spectra.

compete with the intramolecular H-bond, leading to a decrease in tautomer fluorescence yield.⁴ The significantly enhanced tautomer fluorescence of robinetin in HSA as compared to that in water suggests that in the binding pocket of HSA the chromone moiety (which is the part of the molecule mainly relevant to the ESIPT process) of robinetin is comparatively less accessible to water molecules, which facilitates an efficient ESIPT process. This interpretation is further corroborated by the fact that the blue-violet (normal) fluorescence band (which possesses a strong CT character) is dramatically (by $\sim 29 \text{ nm}$) blue-shifted in HSA relative to that obtained in aqueous buffer,

signifying binding to a relatively low polarity environment in the protein matrix where dipolar relaxation is significantly reduced. The emission spectrum of robinetin in aqueous medium consists of overlapping dual fluorescence bands (with the overlap presumably arising due to a solvatochromic red shift of the normal fluorescence⁹) consisting of the tautomer and normal (non-proton-transferred) emissions (with $\lambda_{\text{em}}^{\max}$ ca. 483 and 528 nm, respectively; Figure 2 and Table 1). The strong dependence of the normal fluorescence energy of robinetin and related flavonols (possessing strong CT character) on the surrounding microenvironment polarity has been previously noted.^{8,9,37,62}

In the presence of HSA, the excitation profile of robinetin (monitored at 520 nm; Figure 2a) shows a long-wavelength shoulder ($\sim 415 \text{ nm}$), attributable to the anionic species of robinetin, which is consistent with a band observed in a similar position in the deconvoluted absorption spectrum. Selective excitation of the robinetin anion (by selecting λ_{ex} as 420 nm) results in emission at 495 nm (Figure 2a). Heterogeneity in the ground state species of robinetin in the presence of HSA is further evident from Figure 2b which shows the dependence of the excitation spectrum of robinetin on the emission wavelength. From this, together with the deconvoluted excitation spectrum, presented in Figure 2c, it appears that a significant population of robinetin molecules is in an environment which presumably contains basic amino acid side chain residues, facilitating proton abstraction from robinetin to form ground state anionic species near neutral pH.

Fluorescence anisotropy (r) serves as a sensitive indicator for probing fluorophore binding to motionally constrained regions of proteins.⁵⁴ Figure 3a demonstrates the variations of the steady state fluorescence anisotropy (r) of the ESIPT tautomer with increasing HSA concentration.

The pronounced increase in the “ r ” values of robinetin in the presence of HSA ($r \approx 0.3$ in the presence of $[\text{HSA}] = 10 \mu\text{M}$ whereas $r \approx 0.032$ in aqueous buffer) suggests its binding to motionally constrained site(s) in the protein matrix (Table 1). It appears that the increase in anisotropy saturates at a [robinetin]/[HSA] ratio of 1, indicating a 1:1 stoichiometry for the complex (Figure 3a).⁵⁴ Evidence for neutral species of robinetin strongly bound to HSA is further corroborated from the excitation anisotropy spectra (a plot of steady state fluorescence anisotropy versus excitation wavelength).⁵⁴ The observed dependence of fluorescence anisotropy with excitation wavelength (Figure 3b) is due to the selective excitation and emission of robinetin neutral species bound to motionally constrained site(s) in the HSA matrix.

The occurrence of a substantial amount of ground state anionic species of robinetin in the presence of HSA is clearly evident from the absorption as well as fluorescence emission and excitation spectra discussed earlier (Figures 1 and 2a–c). Presumably, robinetin binds at a site predominantly rich in amino acids that can act as proton acceptors at the specific pH used (pH 7.4). Because robinetin contains an electron

Table 1. Steady State Absorption and Emission Parameters of Robinetin in Aqueous Medium and in the Presence of HSA

medium	$\lambda_{\text{abs}}^{\max}$ (nm)	$\lambda_{\text{em}}^{\max}$ (nm)	blue-violet (I_{I}) ^a	yellow-green (I_{II}) ^a	$I_{\text{II}}/I_{\text{I}}^{\text{a}}$	fluorescence anisotropy (r) ^b
robinetin in aq. buffer	360	483		528	1.72	0.032
robinetin + 25 mM HSA	365	454		548	4.36	0.31

^aComponent peak positions and their ratio from deconvoluted spectra. ^b $\lambda_{\text{ex}} = 380 \text{ nm}$; $\lambda_{\text{em}} = 575 \text{ nm}$.

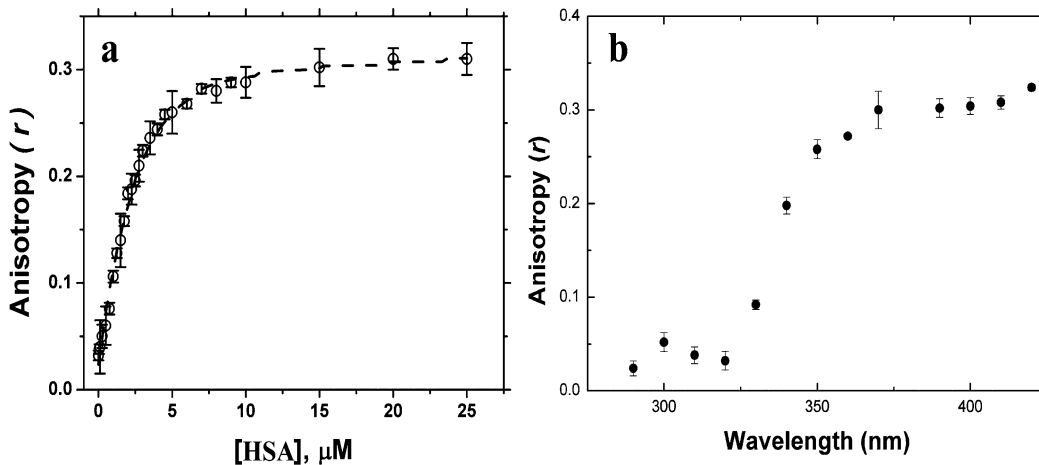


Figure 3. (a) Variation in the fluorescence anisotropy (*r*) of robinetin (10 μM) with increasing protein (HSA) concentration ($\lambda_{\text{ex}} = 380 \text{ nm}$; $\lambda_{\text{em}} = 575 \text{ nm}$). (b) Excitation anisotropy spectra ($\lambda_{\text{em}} = 575 \text{ nm}$) of robinetin (10 μM) in the presence of 25 μM HSA.

Table 2. Fluorescence Decay Parameters of Robinetin (rob) ESIPT Tautomer Emission in Aqueous Buffer and in the Presence of HSA^a

sample	λ_{em} (nm)	α_1	τ_1 (ns)	α_2	τ_2 (ns)	α_3	τ_3 (ns)	$\bar{\tau}$ (ns)	χ^2	DW
rob in water	525	0.998	0.01	0.002	0.79			0.12	1.14	1.85
rob + 20 μM HSA	550	0.38	0.76	0.54	2.22	0.08	5.05	2.60	0.99	1.87

^a[rob] = 10 μM ; $\lambda_{\text{ex}} = 375 \text{ nm}$.

withdrawing C=O group adjacent to the -OH group, it can be expected to behave as a weak acid making proton abstraction and the consequent generation of the anionic species in HSA environment.

Fluorescence lifetime is a sensitive monitor of the local environment of fluorophores. In general, an increase in polarity of the fluorophore environment is known to reduce the lifetime due to fast deactivating processes in polar environments.^{54,63} Fluorescence decay parameters for ESIPT tautomer fluorescence of robinetin in the absence and presence of HSA together with relevant statistical parameters used to check the goodness of fit are shown in Table 2. Interestingly, the average fluorescence lifetime for ESIPT tautomer fluorescence of robinetin increases dramatically from $\sim 0.11 \text{ ns}$ in water to 2.62 ns in HSA, which can be attributed to a decrease in nonradiative decays in the protein matrix. This observation can be rationalized in terms of decreased water exposure in the hydrophobic region of the HSA binding pocket. The fact that the average fluorescence lifetimes as well as the individual components of the fluorescence decay are significantly different from those in water confirms that the robinetin molecules extensively bind with HSA.

From the time-resolved anisotropy decay (Figure 4) combined with eq 5 we estimated the value of rotational correlation time, τ_{rot} . The dramatic increase in τ_{rot} (by >166 times) from $\sim 0.17 \text{ ns}$ in methanol to $\sim 29 \text{ ns}$ in HSA indicates that the precursor of the ESIPT tautomer species is strongly bound in the hydrophobic pocket of HSA where free rotational dynamics is inhibited during the fluorescence lifetime of the flavonoid. The large increase in τ_{rot} is reminiscent of our recent study on the binding of fisetin (a flavonol of related interest) with quadruplex DNA, where ~ 80 times increase in the value of τ_{rot} was noted.²⁷ Methanol rather than water was chosen as a reference protic solvent for comparison because extremely poor solubility and low emission yield of robinetin in water precludes

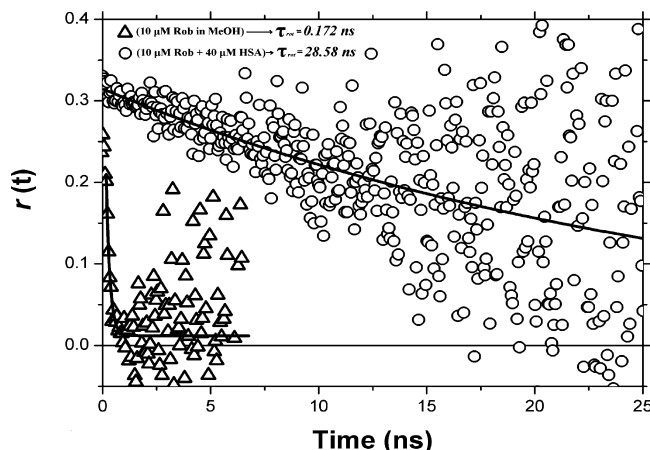


Figure 4. Fluorescence anisotropy decay *r*(*t*) for the robinetin tautomer in the presence (○) and absence (Δ) of HSA at 25 $^{\circ}\text{C}$ where the solid lines are the single exponential fit curve.

meaningful measurements to be performed for aqueous solutions.

Fluorescence contour maps have become a useful tool to investigate protein–ligand interactions. For robinetin in aqueous buffer, the contour plot shows a broad emission band at $\sim 500 \text{ nm}$ for three different excitation wavelengths (260, 325, and 375 nm) due to two separate overlapping fluorescence bands with emission maxima at ~ 485 and $\sim 525 \text{ nm}$ (Figure 5a).

In contrast, for robinetin–HSA complex, the contour plot (Figure 5b) shows well separated dual emission characteristics with emission maxima at ~ 545 and $\sim 480 \text{ nm}$. The substantial difference in the spectral features of the two contour plots (Figure 5a,b) reflects changes in the microenvironment of robinetin upon binding to HSA. Additionally, we notice emission from robinetin upon exciting TRP-214, indicating

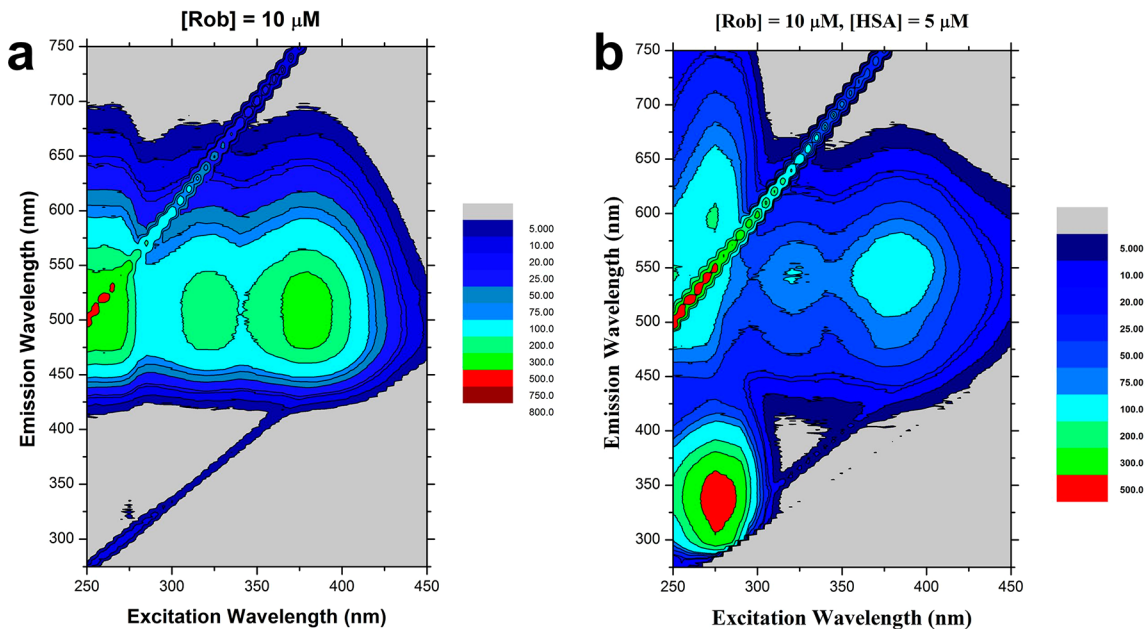


Figure 5. Contour plots of robinetin fluorescence (a) in the absence and (b) in the presence of HSA, in 10 mM pH 7.4 phosphate buffer.

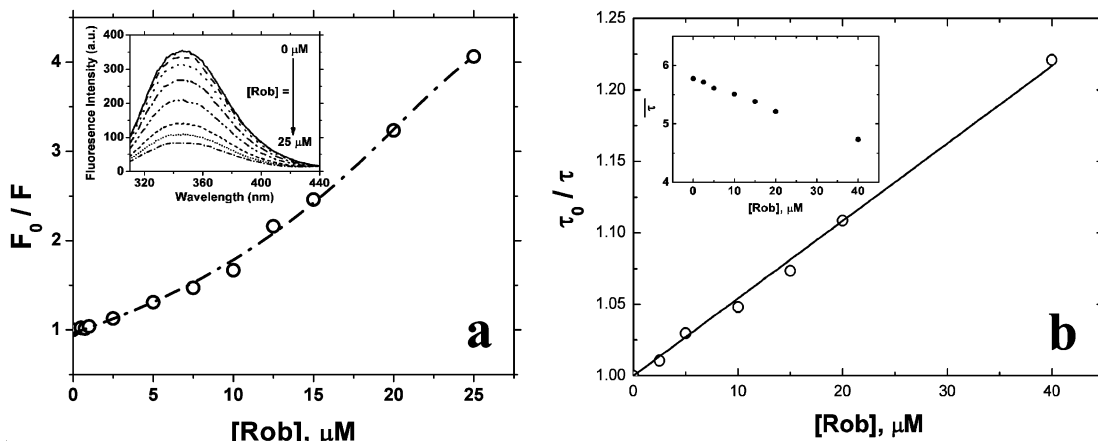


Figure 6. (a) Intensity Stern–Volmer (F_0/F versus [robinetin]). (b) Lifetime Stern–Volmer (τ_0/τ versus [robinetin]) plots for the quenching of the HSA tryptophan fluorescence by robinetin. Inset: (a) Emission spectra of HSA ($\lambda_{\text{ex}} = 295 \text{ nm}$) at 25 °C with varying concentrations of robinetin. (b) Variation of average decay time of HSA tryptophan fluorescence as a function of robinetin concentration.

occurrence of FRET, from the unique TRP-214 residue of HSA to the protein bound robinetin. This is consistent with the fact that FRET is also evident from the fluorescence excitation spectrum of robinetin in the presence of HSA (see Figure 2b,c).

3.1.2. HSA Tryptophan Fluorescence Studies. Quenching of protein tryptophan fluorescence by ligands is a convenient means for exploring ligand–protein interactions.^{39,49–54} Figure 6a (inset) shows quenching of HSA fluorescence in the presence of increasing concentrations of the flavonoid. Figure 6a presents corresponding Stern–Volmer plots based on the equation

$$\frac{F_0}{F} = 1 + K_{\text{SV}}[\text{robinetin}] \quad (7)$$

where F_0 and F denote the fluorescence intensities in the absence and presence of the quencher, respectively, K_{SV} ($=K_q\tau_0$) is the Stern–Volmer (SV) quenching constant for the quenching of HSA tryptophan fluorescence by the flavonoid, K_q is the bimolecular quenching rate constant, and

τ_0 is the average lifetime of the molecule in the excited state in the absence of quencher.⁵⁴ If the SV plot is linear, only a single type of quenching mechanism, i.e., only a static or dynamic type of quenching, is involved, but if the plot shows an upward curvature, the presence of both static and dynamic quenching processes can be inferred^{54,64} Thus, the upward curvature in the intensity Stern–Volmer plot noted here (Figure 6a) signifies the presence of both static and dynamic quenching modes (at the robinetin concentrations used in the present study).

The K_{SV} value estimated from the linear portion of the SV plot is ca. $(58.23 \pm 3.1) \times 10^3 \text{ M}^{-1}$ which is too large to be due to collisional quenching of HSA tryptophan fluorescence by robinetin, especially for an unquenched lifetime (τ_0) of tryptophan ca. 2.7 ns. For a τ_0 value of 2.7 ns, the value of the bimolecular quenching constant, K_q , is found to be $(21.56 \pm 0.86) \times 10^{12} \text{ M}^{-1} \text{ s}^{-1}$ which is nearly 1000-fold larger than the maximum value possible for diffusion-limited quenching in water ($2.0 \times 10^{10} \text{ M}^{-1} \text{ s}^{-1}$).⁵⁴ This large K_q value can be attributed to a static quenching process associated with a

Table 3. Fluorescence Decay Parameters of HSA (Trp-214) in Buffer and in the Presence of Increasing Concentration of Robinetin (rob, Quencher)^a

sample	τ_1 (ns)	τ_2 (ns)	τ_3 (ns)	a_1	a_2	a_3	$\bar{\tau}$ (ns)	χ^2	DW
HSA in aq. buffer	0.36	3.39	6.80	0.18	0.36	0.46	5.77	1.09	1.84
HSA + 20 μM rob	0.46	2.61	6.56	0.28	0.37	0.35	5.21	1.02	1.86
HSA + 40 μM rob	0.57	2.52	6.56	0.37	0.38	0.25	4.71	1.0	1.84

^a[HSA] = 20 μM . Buffer = pH 7.4 (0.01 M) phosphate buffer. Instrument parameters: $\lambda_{\text{ex}} = 295 \text{ nm}$; $\lambda_{\text{em}} = 340 \text{ nm}$; fwhm $\approx 760 \text{ ps}$.

ground state complex formation of robinetin with HSA, due to some specific interaction that increases the local concentrations of the flavonoid around the tryptophan-214 residue in HSA.

Fluorescence lifetime studies were performed in order to obtain further insights regarding the nature of the quenching process. In this connection it may be mentioned that although the presence of a positive deviation from linearity in the SV plot provides the first indication of the existence of both static and dynamic quenching processes, fluorescence lifetime measurements provide the most definitive confirmation regarding the involvement of dynamic mechanisms in the quenching process.^{54,64,65} For static quenching the complexed fluorophores are nonfluorescent, and the only observed fluorescence arises from the uncomplexed fraction. Therefore, the lifetime of the uncomplexed fluorophores (τ_0) remains unchanged and consequently $\tau_0/\tau = 1$ (τ is the lifetime in the presence of quencher). By contrast, for dynamic quenching, $\tau_0/\tau = F_0/F$ where F_0 and F are the fluorescence intensities in the absence and presence of quencher, respectively⁵⁴). Table 3 presents the protein tryptophan fluorescence decay parameters and the effect of addition of robinetin on these parameters.

It is apparent that the lifetime data can be fitted to three exponential decays of HSA both without and with robinetin added (up to a HSA:robinetin molar ratio of 1:2). The decay parameters of HSA (in the absence of the added flavonol) are comparable to those reported by previous workers.⁴⁹ Following a well accepted rotamer model of tryptophan, the three exponential decay components of HSA (see Table 3) are generally attributed to three possible conformations of tryptophan in HSA.⁴⁹ It can be seen that addition of robinetin induces changes in the decay parameters of all three lifetime components of HSA; in view of the complex nature of the decay kinetics, it seemed reasonable to calculate the average fluorescence lifetime and assess the effect of addition of robinetin on this average lifetime value. It is evident that significant decrease occurs in the average fluorescence lifetime ($\bar{\tau}$) of HSA in the presence of robinetin (quencher) (from 5.77 ns, in the absence of robinetin, to 4.71 ns at a [HSA]:[robinetin] molar ratio of 1:2). Such a decrease in the $\bar{\tau}$ value confirms that besides static quenching, a dynamic component is also present as a key mechanism in the observed tryptophan fluorescence quenching process. We attribute this dynamic process to a FRET from the unique tryptophan (TRP-214) residue of HSA to robinetin. This proposal is consistent with the appearance of peaks corresponding to tryptophan absorption noted in the fluorescence excitation spectra (Figure 2b,c) and in the contour plot (Figure 5b), which clearly indicate the occurrence of FRET, as discussed in the preceding section. The dynamic and static portions of the quenching are characterized by the following expressions:⁵⁴ $\tau_0/\tau = 1 + K_D[\text{robinetin}]$ and $(F_0/F)/(\tau_0/\tau) = 1 + K_s[\text{robinetin}]$, where K_D and K_s represent the dynamic and static quenching constants, respectively. K_D has been calculated from a plot of τ_0/τ versus [robinetin] (Figure 6b) and is found to be 5.42 \times

10^3 M^{-1} . The quantity $(F_0/F)/(\tau_0/\tau)$ reflects only the static component of the quenching.⁵⁴ The slope of the plot of $(F_0/F)/(\tau_0/\tau)$ versus [robinetin] (Figure 7) yields the K_s , which in this case represents the association constant for robinetin–HSA interaction,⁵⁴ and is found to be $(5.59 \pm 0.02) \times 10^4 \text{ M}^{-1}$.

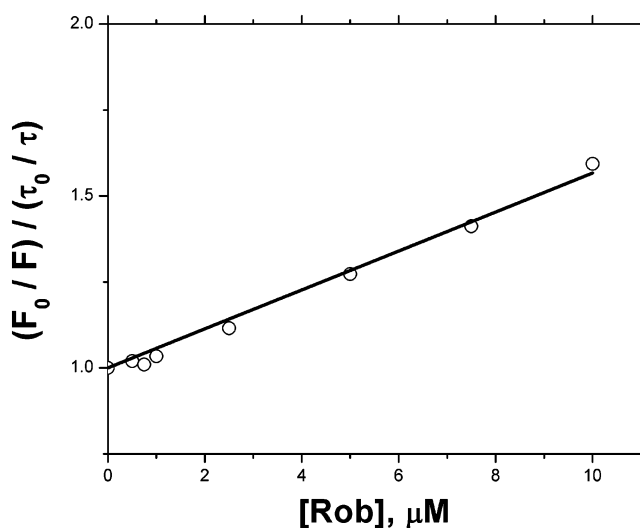


Figure 7. Plot of $(F_0/F)/(\tau_0/\tau)$ versus [robinetin].

It is noteworthy that this value for the association constant happens to be of the same order of magnitude as that observed for the interactions of other structurally related flavonoids with serum albumins and hemoglobin.^{15,33,40} In order to infer the nature of the robinetin–HSA ground state complex in terms of the noncovalent forces involved in the association process, we determined relevant thermodynamic parameters by using the van't Hoff equation:⁶⁶

$$\ln K_a = -\frac{\Delta H}{RT} + \frac{\Delta S}{R} \quad (8)$$

$$\Delta G = \Delta H - T\Delta S \quad (9)$$

Here ΔH , ΔS , and ΔG are the standard enthalpy change, standard entropy change, and standard free energy change, K_a is the binding (association) constant (at the particular temperature used), and R is the gas constant.

From the $\ln K_a$ versus $1/T$ plot presented in the Supporting Information (Figure S1), the values of ΔH and ΔS were determined. ΔG was then calculated. The calculated values of the thermodynamic parameters are listed in Table 4.

From the table, it can be seen that the value of ΔH is strongly negative and ΔS is also negative (Table 4). This indicates that the binding of robinetin with HSA results from the initial involvement of van der Waals interactions between robinetin and HSA molecules, followed by extensive hydrogen bonding interactions between them. A high negative ΔH value also suggests the presence of an electrostatic interaction in the

Table 4. Binding Constant K_a and Related Thermodynamic Parameters of Robinetin–HSA Complex Formation

T (K)	K_a (M^{-1})	ΔG (kcal mol $^{-1}$)	ΔH (kcal mol $^{-1}$)	ΔS (cal mol $^{-1}$ K $^{-1}$)
293	6.84×10^4	-6.48		
298	3.02×10^4	-6.11	-39.15	-112.29
303	7.41×10^3	-5.37		

complexation process. In order to further explore thermodynamic and related aspects, future studies via calorimetric techniques are being contemplated on robinetin and other flavonoids of relevant interest, to obtain detailed insights on how the structure, as well as substituents on the flavones moiety, influences the flavonoid–HSA binding process.

3.1.3. Far- and Near-UV Circular Dichroism Spectroscopic Studies. To further characterize the robinetin–HSA interaction, CD spectroscopic studies have been performed. To investigate the possible effect of the flavonoid binding on the secondary structure of HSA, we used far-UV–CD spectroscopy. The CD spectrum of HSA in aqueous buffer (in the absence of flavonoids) has two characteristic peaks of negative ellipticity at 208 and 222 nm, corresponding to the parallel component of the excitonically split ($\pi - \pi^*$) transition and the ($n - \pi^*$) transition of the peptide group, respectively, indicating its predominantly α -helical secondary structure.⁶⁶ It is found that the CD spectral signature of HSA shows no appreciable change upon addition of different concentrations of robinetin (at fixed HSA concentration of $10 \mu M$) up to $5 \times 10^{-5} M$ (Figure 8a), implying that binding of robinetin causes no significant perturbation of the secondary structure of the protein.

Induced circular dichroism (ICD) spectroscopy in the near-UV region provides crucial and discriminating evidence for the binding of achiral ligands to chiral hosts. Interestingly, prominent ICD bands are noted in the electronic absorption regions of robinetin (an intrinsically achiral molecule) upon binding with HSA (Figure 8b). This indicates that the electronic transitions of the flavonol are strongly perturbed in the chiral binding environment of the protein. The present observation is reminiscent of earlier studies on the interaction of HSA with the monohydroxy flavonoid 7-HF and the polyhydroxy flavonoid quercetin reported by us⁶⁷ and by Zsila et al.,⁶⁸ respectively.

3.2. Docking Studies. HSA is capable of binding to a large number of ligands, including several drugs, with considerable

affinity.^{39,48} All of these compounds bind either at Sudlow's site I, located in subdomain IIA, or at Sudlow's site II, positioned in subdomain IIIA.⁶⁹ In order to explore if robinetin exhibits any binding preference toward any of these sites, we performed a blind docking where the grid size chosen was sufficiently large enough to cover both of the binding sites. The lowest energy docked structure reveals that robinetin binds at site I (Figure 9), commonly known as the warfarin binding site.⁷⁰ It is



Figure 9. Structure of the lowest energy docked complex. HSA is shown in ribbon representation and robinetin is rendered in CPK mode. Nearby TRP-214 is also rendered in magenta CPK representation.

noteworthy that robinetin and warfarin both share highly similar structural scaffolds. In addition, the binding preference of robinetin toward site I obtained from this study is consistent with previous studies on other flavonoids of related interest.^{71–73} Another interesting observation is the presence of the TRP-214 residue in close proximity to the flavonoid binding site (Figure 9). This observation is consistent with the fluorescence quenching of TRP-214 by robinetin.

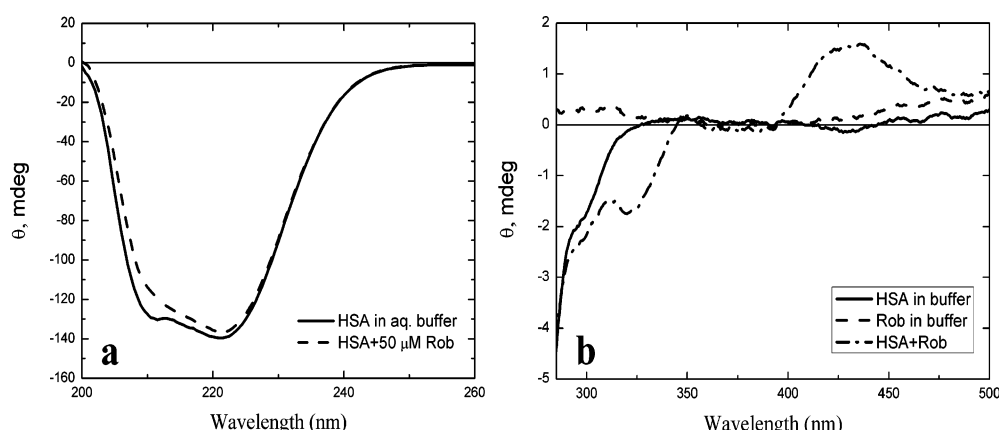


Figure 8. (a) Far-UV CD spectra of HSA in aqueous buffer and the presence of varying concentrations of robinetin. (b) Induced CD spectrum of robinetin ($20 \mu M$) in the presence of HSA. The spectra of robinetin and HSA (in aqueous buffer) are included for comparison.

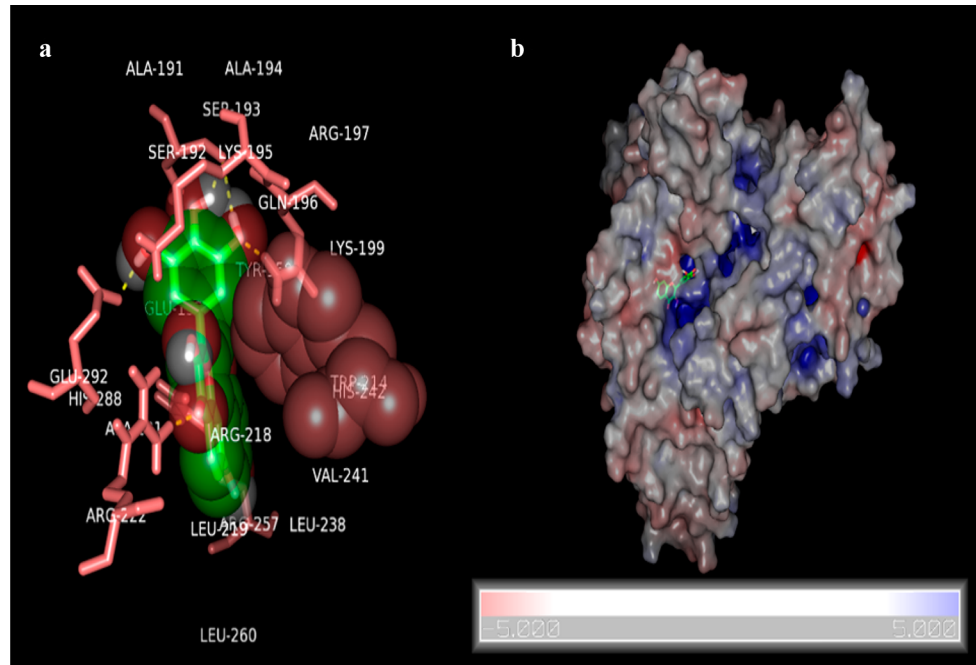


Figure 10. (a) Interaction profile of robinetin within HSA binding site. Robinetin is rendered in both CPK and stick representations while hydrogen bonded residues are shown as sticks. All the other residues within 5 Å are labeled, and TRP-214 is rendered in magenta CPK representation. (b) Electrostatic surface potential of HSA–robinetin complex. Bound robinetin is shown in stick representation. Blue and red colors are used to indicate the most positive and negative electrostatic potentials, respectively.

Moreover, this binding site is mostly hydrophobic which facilitates efficient ESIPT. It is noteworthy that the ESIPT coordinate along C(4)=O···HO-C(3) is well preserved in this binding pose. It is also notable that in this binding pose, robinetin is not planar; rather its B-ring is slightly tilted over the chromone plane allowing efficient hydrogen bonding with the nearby binding site residues.

Figure 10a reveals that robinetin forms seven hydrogen bonds with nearby residues of the HSA binding pocket. 7-OH of robinetin forms a strong hydrogen bond with ARG 257. C(4)=O is involved in hydrogen bonding interactions with ARG 222. 3'-OH shows two hydrogen bonding interactions with GLU 292 and LYS 195. SER 192 of HSA is involved in two hydrogen bonding interactions with both 4'-OH and 5'-OH of robinetin. 5'-OH of robinetin is also involved in additional hydrogen bonding interaction with GLN 196. In this binding pose robinetin displays good steric compatibility in size and shape with the binding site residues of the site I of HSA, leading to a tighter complex formation. This observation can rationalize the observed increase in anisotropy and greatly enhanced rotational correlation time of robinetin upon binding with HSA.

Calculation of electrostatic surface potential using the Poisson–Boltzmann equation (Figure 10b) reveals that the opening of the site I binding pocket of HSA is predominantly positively charged due to the presence of several positively charged residues, Lys 195, ARG 197, LYS 199, ARG 218, HIS 242, ARG 257, and HIS 288. Within the protein interior, histidine presumably exists in deprotonated form which is capable of abstracting hydrogen from robinetin. The anionic form of robinetin molecules thus formed is stabilized in the positively charged region of the binding pocket of HSA. The consequence of the dramatically higher dielectric constant of the HSA binding pocket is that the energy of singly charged robinetin anion in HSA is significantly lower than that in

aqueous solution. This difference in energy (ΔE) can be treated as a perturbation to the dissociation constant by⁶⁶

$$\Delta pK_a = \frac{\Delta E}{2.303k_B T}$$

Consequently, the pK_a for a robinetin buried in the positive electrostatic potential of the HSA pocket should be lower than that in aqueous solution.

4. SUMMARY AND CONCLUDING REMARKS

(i) The present research on robinetin–HSA interaction exemplifies the utility of the exquisitely sensitive “two color” intrinsic fluorescence of flavonols (arising from a photoinduced ESIPT reaction), together with quenching studies of the intrinsic protein (tryptophan) fluorescence, for multiparametric sensing of protein–flavonol interactions.

(ii) Protein binding leads to conspicuous changes in the emission profile of the flavonol, along with a large increase in the ESIPT tautomer fluorescence anisotropy, lifetime, and rotational correlation time (evaluated from time-resolved anisotropy decay studies). Concomitantly, the normal (CT) fluorescence of the flavonol is dramatically (by 29 nm) blue-shifted (corresponding to a decrease in dipolar relaxation effects) in the protein environment. These spectroscopic findings, along with molecular docking studies, are consistent with the picture that the flavonol binds to a motionally constrained, hydrophobic binding site (Sudlow’s site 1) in subdomain IIA of HSA.

(iii) In addition to the intrinsic ESIPT of the flavonol, the occurrence of ground state proton transfer is also evident, presumably due to the presence of proton abstracting side chains of the amino acid(s) in the flavonol binding site in the protein matrix. The latter is evident from the presence of bands corresponding to the anionic species, in the absorption,

fluorescence emission, and excitation profiles, and supported by docking calculations.

(iv) The observation of prominent induced CD (ICD) bands in the near-UV region confirms binding of robinetin in the HSA matrix (where its achiral environment perturbs the electronic structure of the flavonol), while far-UV CD spectra indicate that robinetin binding does not perturb the secondary structure of the protein.

(v) The spectroscopic studies described here, together with the molecular modeling calculations, provide critical insights regarding the binding characteristics of robinetin in the protein (HSA) matrix, offering perspectives for the application of this flavonol as a sensitive multiwavelength fluorescence probe. We can envision promising extension of this research, to other flavonoid derivatives in relation to their binding with different serum albumins as well as other proteins. This may be expected to "open the door" to new avenues for the "screening and design" of the most suitable flavonoid derivatives from among numerous structural variants of this new generation of rapidly emerging phytochemically based drugs, which have strong prospects as viable alternatives to conventional therapeutics.

■ ASSOCIATED CONTENT

Supporting Information

Text describing the number of binding sites and the binding constant and accompanying references and a figure showing the intensity Stern–Volmer plot, binding constant estimation, and the van't Hoff plot. This material is available free of charge via the Internet at <http://pubs.acs.org>.

■ AUTHOR INFORMATION

Corresponding Author

*Fax: 091-033-2351-9755. Tel: 091 9831393962. E-mail: pradeepsinp@yahoo.co.in

Notes

The authors declare no competing financial interest.

■ ACKNOWLEDGMENTS

Dedicated to the memory of Professor Michael Kasha. P.K.S. thanks UGC (India) for the award of an Emeritus Fellowship. We are grateful to the Biophysics & Structural Genomics Division of SINP for use of steady state spectroscopic and associated facilities. We thank Mr. Ajoy Das of the CSD division, SINP and Mr. Subrata Das of the Department of Spectroscopy, IACS for assistance with fluorescence lifetime and time-resolved anisotropy decay measurements. B.P.P. was a postdoctoral fellow at SINP during this work.

■ REFERENCES

- Andersen, O. M., Markham, K. R., Eds. *Flavonoids: Chemistry, biochemistry and applications*; CRC Press: Boca Raton, FL, USA, 2006.
- Harborne, J. B.; Williams, C. A. Advances in Flavonoid Research Since 1992. *Phytochemistry* **2000**, *55*, 481–504.
- Sengupta, P. K.; Kasha, M. Excited State Proton-Transfer Spectroscopy of 3-Hydroxyflavone and Quercetin. *Chem. Phys. Lett.* **1979**, *68*, 382–385.
- Kasha, M. Proton-Transfer Spectroscopy. Perturbation of the Tautomerization Potential. *J. Chem. Soc., Faraday Trans. 2* **1986**, *82*, 2379–2392.
- Demchenko, A. P.; Ercelen, S.; Rosenthal, A. D.; Klymchenko, A. S. Excited-State Proton Transfer Reaction in a New Benzofuryl 3-hydroxychromone Derivative: The Influence of Low-Polar Solvents. *Polym. J. Chem.* **2002**, *76*, 1287–1299.

- Demchenko, A. P. *Introduction to Fluorescence Sensing*; Springer Science + Business Media B. V.: Berlin, 2009.

- Ameer-Beg, S.; Ormsen, S. M.; Brown, R. G.; Matousek, P.; Towrie, M.; Nibbering, E. T. J.; Foggi, P.; Neuwahl, F. V. R. Ultrafast Measurements of Excited State Intramolecular Proton Transfer (ESIPT) in Room Temperature Solutions of 3-Hydroxyflavone and Derivatives. *J. Phys. Chem. A* **2001**, *105*, 3709–3718.

- Sytnik, A.; Gormin, D.; Kasha, M. Interplay Between Excited-State Intramolecular Proton Transfer and Charge Transfer in Flavonols and Their Use as Protein-Binding-Site Fluorescence Probes. *Proc. Natl. Acad. Sci. U. S. A.* **1994**, *91*, 11968–11972.

- Guharay, J.; Sengupta, P. K. Excited-State Proton-Transfer and Dual Fluorescence of Robinetin in Different Environments. *Spectrochim. Acta, Part A* **1997**, *53*, 905–912.

- Dennison, S. M.; Guharay, J.; Sengupta, P. K. Excited-State Intramolecular Proton Transfer (ESIPT) and Charge Transfer (CT) Fluorescence Probe for Model Membranes. *Spectrochim. Acta, Part A* **1999**, *55*, 1127–1132.

- Klymchenko, A. S.; Demchenko, A. P. Multiparametric Probing of Intermolecular Interactions with Fluorescent Dye Exhibiting Excited State Intramolecular Proton Transfer. *Phys. Chem. Chem. Phys.* **2003**, *5*, 461–468.

- Chou, P.-T.; Martinez, M. L.; Clements, J. H. The Observation of Solvent-Dependent Proton-Transfer/Charge-Transfer Lasers from 4'-Diethylamino-3-hydroxyflavone. *Chem. Phys. Lett.* **1993**, *204*, 395–399.

- Chou, P.-T.; Pu, S.-C.; Cheng, Y.-M.; Yu, W.-S.; Yu, Y.-C.; Hung, F.-T.; Hu, W.-P. Femtosecond Dynamics on Excited-State Proton/Charge-Transfer Reaction in 4'-N,N-Diethylamino-3-hydroxyflavone. The Role of Dipolar Vectors in Constructing a Rational Mechanism. *J. Phys. Chem. A* **2005**, *109*, 3777–3787.

- Demchenko, A. P.; Tang, K.-C.; Chou, P.-T. Excited-State Proton Coupled Charge Transfer Modulated by Molecular Structure and Media Polarization. *Chem. Soc. Rev.* **2013**, *42*, 1379–1408.

- Chou, P.-T.; Huang, C.-H.; Pu, S.-C.; Cheng, Y.-M.; Liu, Y.-H.; Wang, Y.; Chen, C.-T. Tuning Excited-State Charge/Proton Transfer Coupled Reaction via the Dipolar Functionality. *J. Phys. Chem. A* **2004**, *108*, 6452–6454.

- Rice-Evans, C. A.; Diplock, A. T. Current Status of Antioxidant Therapy. *Free Radicals Biol. Med.* **1993**, *15*, 77–96.

- Brash, D. E.; Havre, P. A. New Careers for Antioxidants. *Proc. Natl. Acad. Sci. U. S. A.* **2002**, *99*, 13969–13971.

- Havsteen, B. H. The Biochemistry and Medical Significance of the Flavonoids. *Pharmacol. Ther.* **2002**, *96*, 67–202.

- Middleton, E., Jr.; Kandaswami, C.; Theoharides, T. C. The Effects of Plant Flavonoids on Mammalian Cells: Implications for Inflammation, Heart Disease, and Cancer. *Pharmacol. Rev.* **2000**, *52*, 673–751.

- Ishige, K.; Schubert, D.; Sagara, Y. Flavonoids Protect Neuronal Cells from Oxidative Stress by Three Distinct Mechanisms. *Free Radicals Biol. Med.* **2001**, *30*, 433–446.

- Mursu, J.; Voutilainen, S.; Nurmi, T.; Tuomainen, T. P.; Kurl, S.; Salonen, J. T. Flavonoid Intake and the Risk of Ischaemic Stroke and CVD Mortality in Middle-Aged Finnish Men: The Kuopio Ischaemic Heart Disease Risk Factor Study. *Br. J. Nutr.* **2008**, *100*, 890–895.

- Guharay, J.; Sengupta, B.; Sengupta, P. K. Protein–Flavonol Interaction: Fluorescence Spectroscopic Study. *Proteins: Struct., Funct., Genet.* **2001**, *43*, 75–81 and references cited therein.

- Chaudhuri, S.; Sengupta, B.; Taylor, J.; Pahari, B.; Sengupta, P. K. Interactions of Dietary Flavonoids with Proteins: Insights from Fluorescence Spectroscopy and Other Related Biophysical Studies. *Curr. Drug Metab.* **2013**, *14*, 491–503 and references cited therein..

- Sengupta, B.; Banerjee, A.; Sengupta, P. K. Interactions of the Plant Flavonoid Fisetin with Macromolecular Targets: Insights from Fluorescence Spectroscopic Studies. *J. Photochem. Photobiol. B* **2005**, *80*, 79–86.

- Banerjee, A.; Sengupta, P. K. Encapsulation of 3-Hydroxyflavone and Fisetin in Beta-Cyclodextrins: Excited State Proton Transfer

- Fluorescence and Molecular Mechanics Studies. *Chem. Phys. Lett.* **2006**, *424*, 379–386.
- (26) Pahari, B.; Sengupta, B.; Chakraborty, S.; Thomas, B.; McGowan, D.; Sengupta, P. K. Contrasting Binding of Fisetin and Daidzein in γ -Cyclodextrin Nanocavity. *J. Photochem. Photobiol., B* **2013**, *118*, 33–41.
- (27) Sengupta, B.; Pahari, B.; Blackmon, L.; Sengupta, P. K. Prospect of Bioflavonoid Fisetin as a Quadruplex DNA Ligand: A Biophysical Approach. *PLoS One* **2013**, *8*, No. e65383.
- (28) Chaudhuri, S.; Banerjee, A.; Basu, K.; Sengupta, B.; Sengupta, P. K. Interaction of Flavonoids with Red Blood Cell Membrane Lipids and Proteins: Antioxidant and Antihemolytic Effects. *Int. J. Biol. Macromol.* **2007**, *41*, 42–48.
- (29) Gutzeit, H. O.; Henker, Y.; Kind, B.; Franz, A. Specific Interactions of Quercetin and Other Flavonoids with Target Proteins Are Revealed by Elicited Fluorescence. *Biochem. Biophys. Res. Commun.* **2004**, *318*, 490–495.
- (30) Shyamala, T.; Mishra, A. K. Ground- and Excited-State Proton Transfer Reaction of 3-Hydroxyflavone in Dimyristoylphosphatidylcholine Liposome Membrane. *Photochem. Photobiol.* **2004**, *80*, 309–315.
- (31) Mohapatra, M.; Mishra, A. K. Photophysical Behavior of Fisetin in Dimyristoylphosphatidylcholine Liposome Membrane. *J. Phys. Chem. B* **2011**, *115*, 9962–9970.
- (32) Sengupta, B.; Banerjee, A.; Sengupta, P. K. Investigations on the Binding and Antioxidant Properties of the Plant Flavonoid Fisetin in Model Biomembranes. *FEBS. Lett.* **2004**, *570*, 77–81.
- (33) Pahari, B.; Chakraborty, S.; Sengupta, P. K. Encapsulation of 3-Hydroxyflavone in γ -Cyclodextrin Nanocavities: Excited State Proton Transfer Fluorescence and Molecular Docking Studies. *J. Mol. Struct.* **2011**, *1006*, 483–488.
- (34) Sengupta, B.; Sengupta, P. K. The Interaction of Quercetin with Human Serum Albumin: A Fluorescence Spectroscopic Study. *Biochem. Biophys. Res. Commun.* **2002**, *299*, 400–403.
- (35) Sengupta, B.; Sengupta, P. K. Binding of Quercetin with Human Serum Albumin: A Critical Spectroscopic Study. *Biopolymers* **2003**, *72*, 427–434.
- (36) Pahari, B.; Chakraborty, S.; Chaudhuri, S.; Sengupta, B.; Sengupta, P. K. Binding and Antioxidant Properties of Therapeutically Important Plant Flavonoids in Biomembranes: Insights from Spectroscopic and Quantum Chemical Studies. *Chem. Phys. Lipids* **2012**, *165*, 488–496.
- (37) Banerjee, A.; Basu, K.; Sengupta, P. K. Effect of β -Cyclodextrin Nanocavity Confinement on the Photophysics of Robinetin. *J. Photochem. Photobiol., B* **2007**, *89*, 88–97.
- (38) Jana, B.; Senapati, S.; Ghosh, D.; Bose, D.; Chattopadhyay, N. Spectroscopic Exploration of Mode of Binding of ctDNA with 3-Hydroxyflavone: A Contrast to the Mode of Binding with Flavonoids Having Additional Hydroxyl Groups. *J. Phys. Chem. B* **2012**, *116*, 639–645.
- (39) Dangles, O.; Dufour, C.; Manach, C.; Morand, C.; Remsey, C. Binding of Flavonoids to Plasma Proteins. *Methods Enzymol.* **2001**, *335*, 319–333.
- (40) Xiao, J.; Suzuki, M.; Jiang, X.; Chen, X.; Yamamoto, K.; Ren, F.; Xu, M. Influence of B-Ring Hydroxylation on Interactions of Flavonols with Bovine Serum Albumin. *J. Agric. Food Chem.* **2008**, *56*, 2350–2356.
- (41) Xiao, J.; Cao, H.; Chen, T.; Yang, F.; Liu, C.; Xu, X. Molecular Property-Binding Affinity Relationship of Flavonoids for Common Rat Plasma Proteins in Vitro. *Biochimie* **2011**, *93*, 134–140.
- (42) Birt, D. F.; Walker, B.; Tibbels, M. G.; Bresnick, E. Anti-Mutagenesis and Anti-Promotion by Apigenin, Robinetin and Indole-3-Carbinol. *Carcinogenesis* **1986**, *7*, 959–963.
- (43) Tasdemir, D.; Kaiser, M.; Brun, R.; Yardley, V.; Schmidt, T. J.; Tosun, F.; Rüedi, P. Antitrypanosomal and Antileishmanial Activities of Flavonoids and Their Analogues: In Vitro, In Vivo, Structure-Activity Relationship, and Quantitative Structure-Activity Relationship Studies. *Antimicrob. Agents Chemother.* **2006**, *50*, 1352–1364.
- (44) Manjolin, L. C.; Goncalves dos Reis, M. B.; do Carmo Maquiaveli, C.; Santos-Filho, O. A.; da Silva, E. R. Dietary Flavonoids Fisetin, Luteolin and Their Derived Compounds Inhibit Arginase, a Central Enzyme in *Leishmania (Leishmania) amazonensis* Infection. *Food Chem.* **2013**, *141*, 2253–2262.
- (45) Chaudhuri, S.; Pahari, B.; Sengupta, B.; Sengupta, P. K. Binding of the Bioflavonoid Robinetin with Model Membranes and Hemoglobin: Inhibition of Lipid Peroxidation and Protein Glycosylation. *J. Photochem. Photobiol., B* **2010**, *98*, 12–19.
- (46) Asgary, S.; Naderi, Gh.; Sarrafzadegan, N.; Ghassemi, N.; Boshtam, M.; Rafie, M.; Arefian, A. Anti-Oxidant Effect of Flavonoids on Hemoglobin Glycosylation. *Pharm. Acta Helv.* **1999**, *73*, 223–226.
- (47) Sengupta, B.; Swenson, J. Properties of Normal and Glycated Human Hemoglobin in Presence and Absence of Antioxidant. *Biochem. Biophys. Res. Commun.* **2005**, *334*, 954–959.
- (48) He, X. M.; Carter, D. C. Atomic Structure and Chemistry of Human Serum Albumin. *Nature* **1992**, *358*, 209–215.
- (49) Rolinski, O. J.; Martin, A.; Birch, J. S. D. Human Serum Albumin and Quercetin Interactions Monitored by Time-Resolved Fluorescence: Evidence for Enhanced Discrete Rotamer Conformations. *J. Biomed. Opt.* **2007**, *12*, No. 034013.
- (50) Rolinski, O. J.; Martin, O. A.; Birch, D. J. S. Human Serum Albumin-Flavonoid Interactions Monitored by Means of Tryptophan Kinetics. *Ann. N. Y. Acad. Sci.* **2008**, *1130*, 314–319.
- (51) Singha Roy, A.; Dinda, A. K.; Dasgupta, S. Study of the Interaction Between Fisetin and Human Serum Albumin: A Biophysical Approach. *Protein Pept. Lett.* **2012**, *19*, 604–615.
- (52) Singha Roy, A.; Pandey, N. K.; Dasgupta, S. Preferential Binding of Fisetin to the Native State of Bovine Serum Albumin: Spectroscopic and Docking Studies. *Mol. Biol. Rep.* **2013**, *40*, 3239–3253.
- (53) Chakraborty, S.; Chaudhuri, S.; Pahari, B.; Taylor, J.; Sengupta, P. K.; Sengupta, B. A Critical Study on the Interactions of Hesperitin with Human Hemoglobin: Fluorescence Spectroscopic and Molecular Modeling Approach. *J. Lumin.* **2012**, *132*, 1522–1528.
- (54) Lakowicz, J. R. *Principles of Fluorescence Spectroscopy*, 3rd ed.; Springer-Verlag: New York, 2006.
- (55) Origin; OriginLab: Northampton, MA, USA, 2007.
- (56) Wojdyl, M.; Fityk, A. General-Purpose Peak Fitting Program. *J. Appl. Crystallogr.* **2010**, *43*, 1126–1128.
- (57) Hyperchem; Hypercube: Gainesville, FL, USA, 2002.
- (58) Morris, G. M.; Huey, R.; Lindstrom, W.; Sanner, M. F.; Belew, R. K.; Goodsell, D. S.; Olson, A. J. Autodock4 and Autodock Tools4: Automated Docking With Selective Receptor Flexibility. *J. Comput. Chem.* **2009**, *30*, 2785–2791.
- (59) Jo, S.; Kim, T.; Iyer, V. G.; Im, W. CHARMM-GUI: A Web-Based Graphical User Interface for CHARMM. *J. Comput. Chem.* **2008**, *29*, 1859–1865.
- (60) Im, W.; Beglov, D.; Roux, B. Continuum Solvation Model: Electrostatic Forces from Numerical Solutions to the Poisson-Boltzmann Equation. *Comput. Phys. Commun.* **1998**, *111*, 59–75.
- (61) Jo, S.; Vargyas, M.; Vasko-Szedlar, J.; Roux, B.; Im, W. PBEQ-Solver for Online Visualization of Electrostatic Potential of Biomolecules. *Nucleic Acids Res.* **2008**, *36*, W270–W275.
- (62) Chaudhuri, S.; Chakraborty, S.; Sengupta, P. K. Probing the Interactions of Hemoglobin with Antioxidant Flavonoids via Fluorescence Spectroscopy and Molecular Modeling Studies. *Biophys. Chem.* **2011**, *154*, 26–34.
- (63) Raghuraman, H.; Chattopadhyay, A. Interaction of Melittin with Membrane Cholesterol: A Fluorescence Approach. *Biophys. J.* **2004**, *87*, 2419–2432.
- (64) Mandal, P.; Ganguly, T. Fluorescence Spectroscopic Characterization of the Interaction of Human Adult Hemoglobin and Two Isatins, 1-Methylisatin and 1-Phenylisatin: A comparative Study. *J. Phys. Chem. B* **2009**, *113*, 14904–14913.
- (65) Bardhan, M.; Chowdhury, J.; Ganguly, T. Investigations on the interactions of aurintricarboxylic acid with bovine serum albumin: Steady state/ time resolved spectroscopic and docking studies. *J. Photochem. Photobiol., B* **2011**, *102*, 11–19.

- (66) van Holde, K. E.; Johnson, C.; Ho, P. S. *Principles of Physical Biochemistry*, 2nd int. ed.; Pearson Higher Education: Upper Saddle River, NJ, USA, 2006.
- (67) Banerjee, A.; Basu, K.; Sengupta, P. K. Interaction of 7-Hydroxyflavone with Human Serum Albumin: A Spectroscopic Study. *J. Photochem. Photobiol., B* **2008**, *90*, 33–40.
- (68) Zsila, F.; Bikádi, Z.; Simonyi, M. Probing the Binding of the Flavonoid, Quercetin to Human Serum Albumin by Circular Dichroism, Electronic Absorption Spectroscopy and Molecular Modelling Methods. *Biochem. Pharmacol.* **2003**, *65*, 447–456.
- (69) Sudlow, G.; Birkett, D. J.; Wade, D. N. The Characterization of Two Specific Drug Binding Sites on Human Serum Albumin. *Mol. Pharmacol.* **1975**, *11*, 824–832.
- (70) Petitpas, I.; Bhattacharya, A. A.; Twine, S.; East, M.; Curry, S. Crystal Structure Analysis of Warfarin Binding to Human Serum Albumin: Anatomy of Drug Site I. *J. Biol. Chem.* **2001**, *276*, 22804–22809.
- (71) Barreca, D.; Laganà, G.; Bruno, G.; Magazù, S.; Bellocchio, E. Diosmin Binding to Human Serum Albumin and Its Preventive Action Against Degradation Due to Oxidative Injuries. *Biochimie* **2013**, *95*, 2042–2049.
- (72) Feroz, S. R.; Mohamad, S. B.; Bakri, Z. S. D.; Malek, S. N. A.; Tayyab, S. Probing the Interaction of a Therapeutic Flavonoid, Pinostrubin with Human Serum Albumin: Multiple Spectroscopic and Molecular Modeling Investigations. *PLoS One* **2013**, *8*, No. e76067.
- (73) Bolli, A.; Marino, M.; Rimbach, G.; Fanali, G.; Fasano, M.; Ascenzi, P. Flavonoid Binding to Human Serum Albumin. *Biochem. Biophys. Res. Commun.* **2010**, *398*, 444–449.